SCIENTIFIC REPORTS

OPEN

SUBJECT AREAS:
BATESIAN MIMICRY
TRANSCRIPTIONAL REGULATORY ELEMENTS

Received
26 July 2013

Accepted
25 October 2013

Published
11 November 2013

Correspondence and requests for materials should be addressed to H.F. (haruh@k.u-tokyo.ac.jp)

Molecular basis of wing coloration in a Batesian mimic butterfly, *Papilio polytes*

Hideki Nishikawa[1], Masatoshi Iga[1], Junichi Yamaguchi[1], Kazuki Saito[1], Hiroshi Kataoka[1], Yutaka Suzuki[2], Sumio Sugano[3] & Haruhiko Fujiwara[1]

[1]Department of Integrated Biosciences, Graduate School of Frontier Sciences, The University of Tokyo, Kashiwa, Chiba 277-8562, Japan, [2]Department of Computational Biology, Graduate School of Frontier Sciences, The University of Tokyo, Kashiwa, Chiba 277-8562, Japan, [3]Department of Medical Genome Sciences, Graduate School of Frontier Sciences, The University of Tokyo, Kashiwa, Chiba 277-8562, Japan.

Batesian mimicry protects animals from predators through resemblance with distasteful models in shape, color pattern, or behavior. To elucidate the wing coloration mechanisms involved in the mimicry, we investigated chemical composition and gene expression of the pale yellow and red pigments of a swallowtail butterfly, *Papilio polytes*, whose females mimic the unpalatable butterfly *Pachliopta aristolochiae*. Using LC/MS, we showed that the pale yellow wing regions in non-mimetic females consist of kynurenine and N-β-alanyldopamine (NBAD). Moreover, qRT-PCR showed that kynurenine/NBAD biosynthetic genes were upregulated in these regions in non-mimetic females. However, these pigments were absent in mimetic females. RNA-sequencing showed that kynurenine/NBAD synthesis and *Toll* signaling genes were upregulated in the red spots specific to mimetic female wings. These results demonstrated that drastic changes in gene networks in the red and pale yellow regions can switch wing color patterns between non-mimetic and mimetic females of *P. polytes*.

Animal coloration is an adaptive trait that is often diversified among closely related species. In particular, wing patterns of butterflies vary greatly, and these variations have attracted public as well as researchers and have been studied since the time of Darwin. Among the various strategies used by butterflies to avoid predators, some butterflies have become unpalatable by incorporating plant alkaloids[1] or producing a toxin-like cyanogenic glycoside[2] as defensive chemicals. Unpalatable butterflies inform predators to their toxicity by exhibiting conspicuous wing patterns, such as the unique banding pattern of heliconid butterflies[3]. Some unpalatable butterflies share similar wing patterns to provide mutualistic protection called Mullerian mimicry[4]. In contrast, some palatable butterflies have evolved another strategy called Batesian mimicry: they mimic the conspicuous wing patterns of unpalatable species and acquire protective effects[5–8]. Multiple loci are involved in the expression of Mullerian mimicry phenotypes in heliconid butterflies[9,10], whereas the phenotypes of Batesian mimicry species reported to date are determined by a single locus[11–13]. To elucidate the evolutionary processes of mimicry comprehensively, it is necessary to study the molecular basis of Batesian mimicry.

The swallowtail butterfly *Papilio polytes* is notable for exhibiting female-limited Batesian mimicry[13]. The females have 2 forms: the non-mimetic female (also called *cyrus*), almost identical to monomorphic males that have only pale yellow bands on the hindwings (Fig. 1a, b), and the mimetic female (also called *polytes*), which mimics the distasteful butterfly *Pachliopta aristolochiae*. The latter has centered pale yellow regions and periclinal red spots on the hindwings (Fig. 1c, d). This female dimorphism is controlled by a single autosomal locus *H* and the mimetic phenotype is dominant[13]. The pigmentation processes involved in Batesian mimicry of *P. polytes* are considered to be downstream of the *H* gene; however, the gene activation networks as well as the genes involved in this pigmentation are largely unknown.

Chemical characterization of pigments is necessary for understanding the coloration processes. A few pigments in the butterfly wings have been identified to date. Pterin pigments are found in the wing scales of pierid butterflies[14], and ommochrome pigments are involved in wing coloration in nymphalid and heliconid butterflies[15,16]. Papiliochrome is found mainly in papilionid butterflies, and the NMR spectrum data indicate that the aromatic amino group of kynurenine forms a chemical bond with the β- carbon of the side chain of N-β-alanyldopamine (NBAD) in papiliochrome II[17]. In many papilionid butterflies, papiliochrome II forms the pale yellow pigment[18], but the red pigments have not been characterized chemically. Thus, identifying these pigments both in mimetic and non-mimetic wings of *P. polytes* is necessary for understanding the switching between the 2 phenotypes. Moreover, it would be interesting to analyze the properties of each pigment to solve the evolutionary

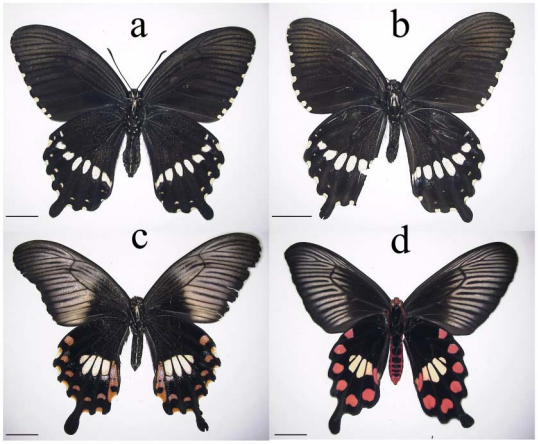

Figure 1 | **Adult wing color patterns of 2 species.** (a) *Papilio polytes*, male. (b) *P. polytes*, non-mimetic female. (c) *P. polytes*, mimetic female. (d) Model butterfly *Pachliopta aristolochiae*. Bars represent 1 cm. All images in this figure were captured by the author (H. Nishikawa).

puzzle: the pigments in the wings of the model butterfly *P. aristolochiae* are used correspondingly in the mimetic females of *P. polytes*.

In this study, we used LC/MS to show that the pale yellow pigments of non-mimetic females consist of kynurenine and NBAD but mimetic females express other types of pigments. In addition, qRT-PCR analysis showed that kynurenine and NBAD synthesis genes are upregulated in the pale yellow regions in non-mimetic females but not in mimetic females. These data suggest that pigment synthesis can be switched on and off, resulting in either mimetic or non-mimetic females. In addition, we found that the red pigments of mimetic females are formed through the polymerization of kynurenine and NBAD compounds in a process potentially associated with novel factors such as the *Toll* signaling pathway.

Results

Comparison of pupal wing coloration in mimetic and non-mimetic females. To characterize the pigmentation processes, we first determined the development of pupal wing patterns. Pupal stages of *P. polytes* lasted for 12 days at 25°C. From immediately after pupation (P0) to 3 days after pupation (P3), epidermal cells outside the bordering lacuna (BL) were present (Fig. 2), but these cells disappeared because of cell death at stage P4[19]. Pupal wing coloration started between P8 and P9. First, pale yellow pattern coloration was observed from P9 to P10. Notably, the pale yellow pattern of mimetic females emerged as a round shape near the wing center, whereas that of non-mimetic females appeared as an extended band. Next, the red spots appeared in the distal regions in mimetic females between P10 and P10.5. Finally, black coloration occurred, and the wing pattern formation completed at stage P11. Coloration in males was almost the same as that in non-mimetic females. Based on the above observations, Fig. S1 summarizes region- and stage-specific coloration for pale yellow, red and black regions during pupal wing development in *P. polytes*.

Identification of the pale yellow pigments using LC/MS analysis. Because the shape and position of the pale yellow region are different between mimetic and non-mimetic females, we first attempted to

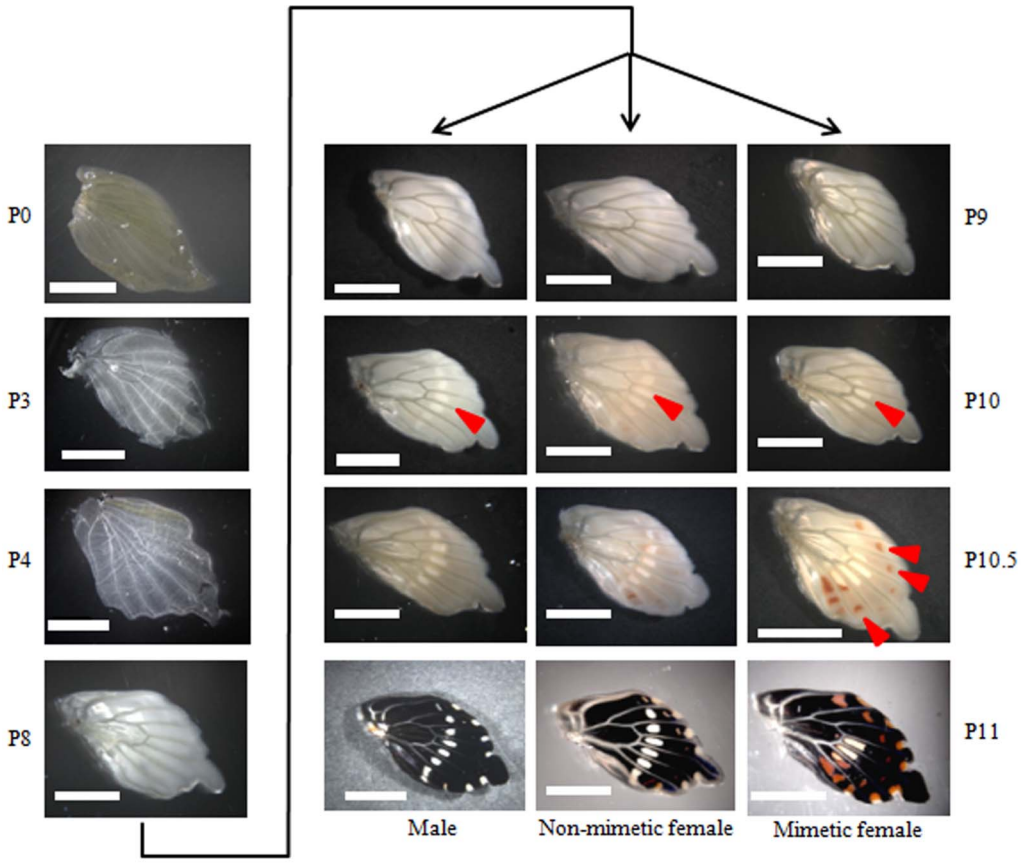

Figure 2 | **Pupal stages for hindwing coloration in *P. polytes*.** P0–P11 show each stage, in days after pupation. P0: immediately after pupation. P8: the wing is covered with scales but pigmentation is not present. P9: pale yellow coloration begins. P10: the shape of the pale yellow region appears clearly. P10.5: the pale yellow pattern appears clearer and red pigment coloration occurs in mimetic female wings. P11: black coloration occurs and all pigmentations are completed. Bars represent 5 mm. All images in this figure were captured by the author (H. Nishikawa).

characterize the pale yellow pigment chemically. The pale yellow pigment, which was extracted from the hindwings of non-mimetic females using 70% methanol, showed 3 main peaks with retention times between 4.5 and 5.5 min on a high-performance liquid chromatography electrospray ionization accurate mass spectrometry (HPLC-ESI-MS) system (Fig. 3a). We named these peaks 1, 2, and 3 in order starting from the peak with the longest retention time. Peak 1 showed the highest intensity in total ion chromatography. The accurate mass spectrum of peak 1 was m/z 431.1929, indicating that the chemical formula of peak 1 was $C_{21}H_{26}N_4O_6$ (Fig. 3b). This chemical composition indicated that the peak 1 substance corresponds to a compound consisting of NBAD and kynurenine moieties: papiliochrome II[17]. The accurate mass spectrum of peaks 2 and 3 was m/z 653.2933 and 875.3944 respectively (Fig. 3c, d), indicating that the chemical formula was $C_{32}H_{40}N_6O_9$ and $C_{43}H_{54}N_8O_{12}$, respectively. MS/MS analysis of peak 2 revealed that this peak includes 2 substances: kynurenine and a molecule with m/z 445.2085 that is equivalent to an NBAD dimer, judging by the molecular weight and chemical composition (Fig. S2). In addition, the accurate molecular weight of peak 3 indicated that it was equivalent to kynurenine and an NBAD trimer (Fig. 3d). These results showed that all 3 peaks correspond to substances composed

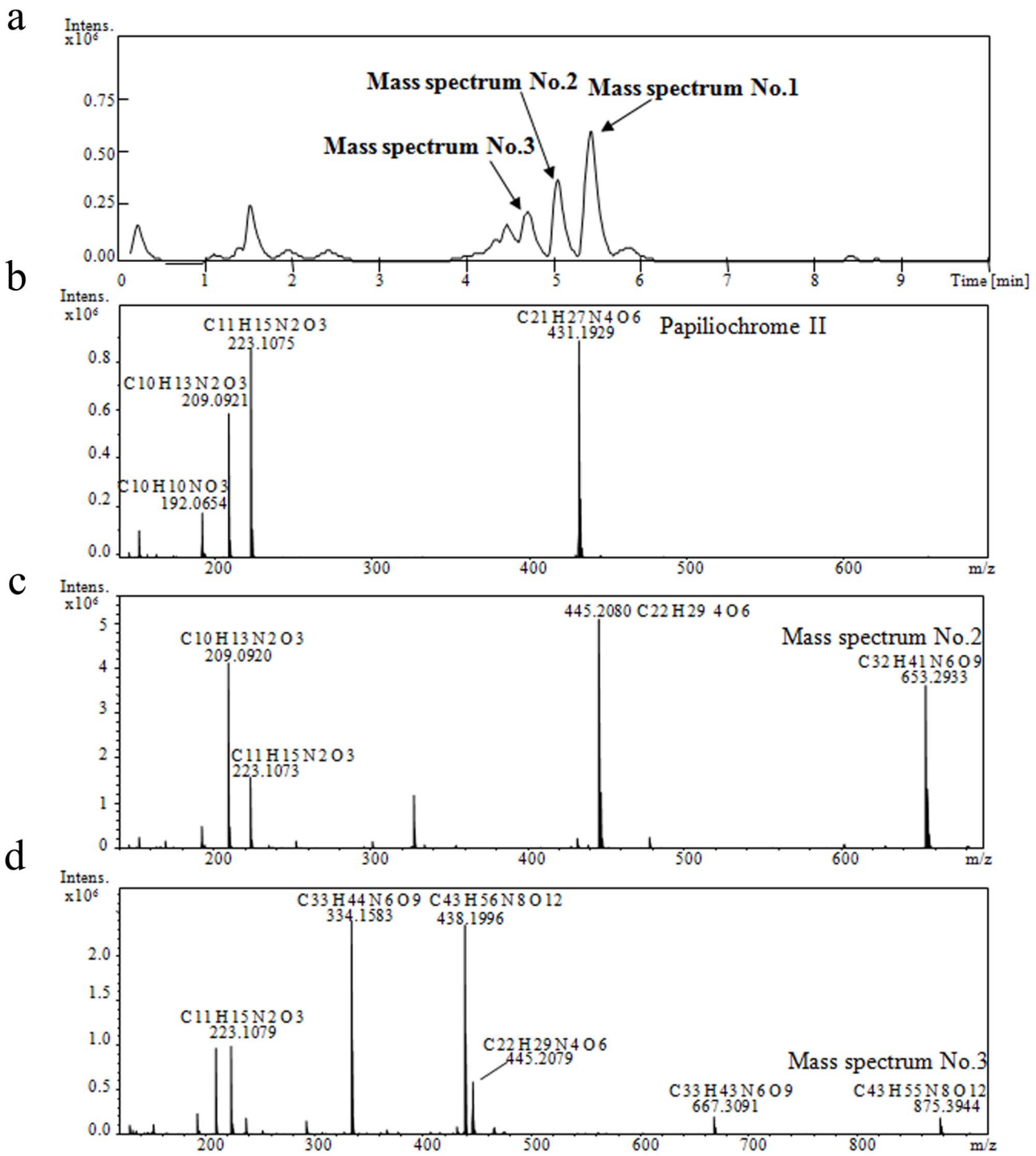

Figure 3 | Liquid chromatography/mass spectrometry analysis of the pale yellow pigments. (a) A chromatogram of the pale yellow pigments shows 3 main peaks 1–3. Mass spectra and chemical composition of peak 1 (b), peak 2 (c), and peak 3 (d).

of kynurenine chemically linked to NBAD (monomer, dimer, or trimer), which mainly serve as pale yellow pigments in non-mimetic females. However, it is not clear whether all 3 substances are necessary for pale yellow coloration and if their amounts are controlled strictly.

We next attempted to isolate the pale yellow pigments from mimetic females using the methods identical to those described above. The chromatogram of the extract from wings of non-mimetic females at 380 nm, the wavelength that showed maximal absorption in the spectrum of papiliochrome II, showed the same 3 peaks as discussed above, and therefore, the pale yellow pigments were present (Fig. S3). However, the pale yellow pigments of mimetic females were not soluble in 70% methanol that was used for dissolving the pale yellow pigments of non-mimetic females. Therefore, these 3 pigments of non-mimetic females were not present in mimetic females (Fig. S4). This observation and further gene expression analysis (see below) indicated that the yellow pigment in mimetic females consist of compounds those were different from the papiliochrome II-related pigments of the non-mimetic females.

Expression patterns of kynurenine and NBAD pathway genes. To determine whether the pale yellow pigments are formed as a result of region-specific expression of genes involved in the synthesis of kynurenine and NBAD, we assessed the expression patterns of these genes. The kynurenine synthesis pathway is known to start with tryptophan that is converted to formylkynurenine by vermilion and further to kynurenine by kynurenine formamidase (kf)[20] (Fig. S5). NBAD is known to be the pigment in the abdominal stripes of *Drosophila melanogaster*[21], and serves as a precursor of cuticle sclerotization[22]. The NBAD synthesis pathway starts with tyrosine that is converted to DOPA by tyrosine hydroxylase (TH) and further to dopamine by DOPA decarboxylase (DDC). Finally, ebony converts dopamine and β-alanine to NBAD[21] (Fig. S5). Therefore, we quantified the expression level of these genes in the 2 pathways by quantitative real-time PCR (qRT-PCR) using mRNAs from the pupal hindwings from P9 to P11. Based on the position of wing veins, we dissected 3 separate areas: future black region, future pale yellow region, and future red spot regions in non-mimetic females (Fig. 4), and mimetic females (Fig. 5). The shapes of the pale yellow regions were different between the 2 types of females, and the red region in non-mimetic females was not evident, but its corresponding region in non-mimetic females was isolated successfully.

Because the *kf* gene has not been identified in *P. polytes*, we first used degenerate PCR primers to clone a partial sequence (551 bp) of the gene (AB857712), whose deduced amino acid sequence shows 85% similarity to the gene of *Heliconius melpomene*. Phylogenetic analysis also indicates that this gene is the *kf* ortholog in *P. polytes* (Fig. S6). Based on this sequence and the sequences of 4 other genes that have been sequenced before, we compared the gene expression patterns in the 3 different regions between non-mimetic and mimetic females.

(1) Similar gene expression profiles in the future black regions

In the hindwings of non-mimetic females, *vermilion* and *kf* from the kynurenine pathway were expressed at relatively low levels in the future black and red spot-corresponding regions (Fig. 4, black and red lines). Because both regions become black, we assumed that these genes are not involved in black region formation, and their similar expression in the future black region in mimetic females supports this notion (Fig. 5, black line). In contrast, transcription of *TH* and *DDC* was upregulated in all future black regions at stage P10.5 and P11 (Fig. 4, black and red lines and Fig. 5, black line), suggesting that these genes when induced at these stages may participate in melanin synthesis in the black regions or in the sclerotization processes in pupal cuticle. We also observed high levels of *ebony* expression at stage P10 and P10.5 in the future black regions (Fig. 4, black line and Fig. 5, black line), whose functional roles are not clear.

(2) Differences in patterns of gene expression in the pale yellow regions between mimetic and non-mimetic females

In the pale yellow region in non-mimetic females, significant changes in gene expression were observed in the kynurenine pathway: transcription of both *vermilion* and *kf* was induced at stage P10 and P10.5 (Fig. 4, blue line). In this region, all genes in the NBAD pathway were also induced at stage P10 and P10.5. These results strongly support the above conclusion that the pale yellow pigment in non-mimetic females is composed of kynurenine and NBAD. Because the pale yellow region in non-mimetic females appears clearly from P10 (Fig. 2), the increased expression level of these genes is consistent with the development timing.

Nonetheless, in the pale yellow region of mimetic female hindwings, we did not observe the induction of the kynurenine pathway genes (Fig. 5, blue line), similar to those in the black region. Expression of NBAD pathway genes was also similar between the pale yellow and black regions in mimetic females (Fig. 5, blue and black lines). Together with the finding that the pale yellow pigments of mimetic females could not be extracted with 70% methanol (Fig. S4), these results indicate that kynurenine or its related substances are absent from in the pale yellow pigment in mimetic females. NBAD synthesis genes were slightly upregulated at P10.5, when the pale yellow pigmentation was completed. Thus, it is possible that NBAD was not involved in the synthesis of the pale yellow pigments in mimetic females. These results suggest that the yellow pigments are synthesized differently and altered between non-mimetic and mimetic females in a region-specific manner.

(3) Stage- and region-specific induction of kynurenine and NBAD pathway genes in the red spots of mimetic wings

The red spots on the hindwings are clearly visible in mimetic females but are barely detectable in non-mimetic females (Fig. 1). Thus, elucidation of the regulation of genes in this region is crucial for understanding the molecular mechanisms underlying Batesian mimicry. In mimetic wings, the expression levels of 4 genes, *vermilion*, *kf*, *DDC*, and *ebony*, but not of *TH*, were specifically increased in the red region at stage P10.5 (Fig. 5, red line), the red pigment synthesis stage (Fig. 2). *TH* was upregulated at stage P11, same as that in the pale yellow and black regions. In contrast, in non-mimetic wings, expression of these genes was not induced in the red spot-corresponding regions of non-mimetic female (Fig. 4, red line). These data suggest that both kynurenine and NBAD synthesis pathways are involved in red pigment synthesis in mimetic wings of *P. polytes*. To confirm this observation, we attempted to investigate the chemical composition of the red pigment; however, we were unable to dissolve the pigment in any organic solvent: methanol, acetone, chloroform, and 4% hydrochloric acid in methanol, suggesting that the red pigment is highly polymerized and stable.

Melanin, known to be insoluble in any organic solvent, is a highly polymerized substance that mainly comprises an indole skeleton[23] and is insoluble in hydrochloric acid. In flesh flies, melanin in the adult integument is not dissolved in hot hydrochloric acid[24]. Thus, we applied this hydrochloric acid treatment and found that the pale yellow regions in non-mimetic females were hydrolyzed and became transparent. In contrast, the red region in mimetic females did not change, same as the black region (melanin pigment) (Fig. S7). These results also suggest that the chemical composition of the red pigment is similar to that of melanin and may polymerize in a similar manner.

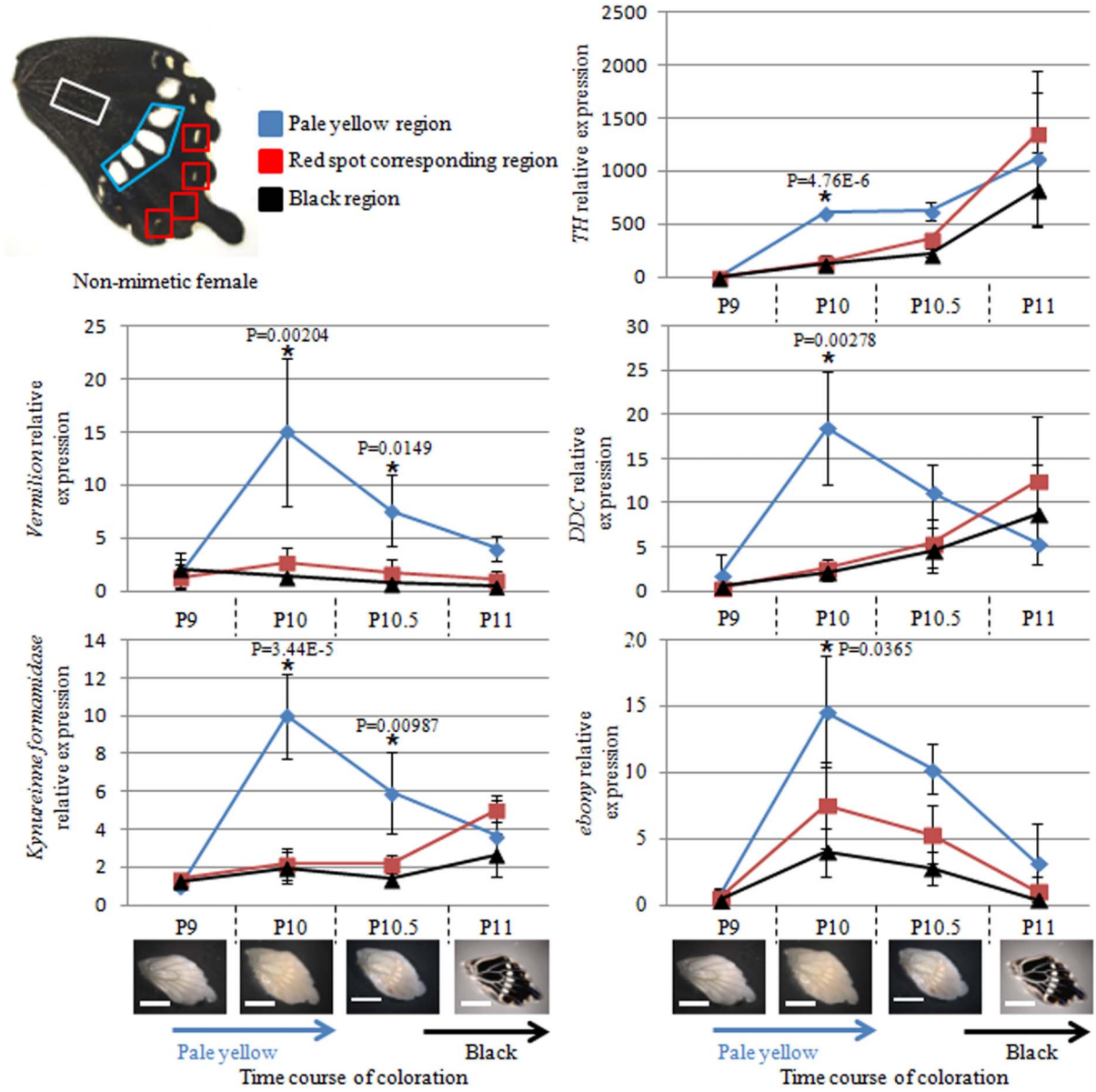

Figure 4 | Expression levels of kynurenine and NBAD pathway genes in the late pupal wings of non-mimetic females. Three separate regions are indicated: blue line, indicating the pale yellow region; red line, indicating the red spots-corresponding region; and black line, indicating the black region. The expression levels of all genes are shown relative to that of the *rpL3* control. Error bars show standard deviation of 3 or 4 experimental replicates. (*$P < 0.05$, one-way ANOVA). All images in this figure were captured by the author (H. Nishikawa).

Comprehensive analysis of genes involved in red pigment synthesis in mimetic wings. To determine the substances that constitute the red pigment in mimetic wings, we performed RNA sequencing to identify genes involved in red pigment synthesis. To compare the red spots on mimetic wings and the red spot-corresponding regions in non-mimetic females at the same stage (P10.5, the red pigment synthesis stage), we prepared RNA from these regions (Fig. 4 and 5, red) of 3 pupae, respectively, for RNA sequencing. All sequence reads were assembled into 79,769 transcripts using Trinity *de novo* transcript assembly software package (accession number: DRZ003159). We compared the gene expression patterns of 2 regions; 373 genes were expressed more in the red spots of mimetic females (Table S2), but 169 genes were expressed more strongly in the red spot-corresponding regions in non-mimetic females (Table S3). The notable genes upregulated in mimetic wings are involved in redox reactions (6 genes), signaling pathway and transcriptional regulation (10 genes), transporter functions (26 genes) and enzymatic activity (50 genes); however, the function of these genes in the formation of the red spots is unclear.

The expression levels (reads per kilobase of exons per million mapped reads [RPKM] values) of the kynurenine pathway genes *vermilion* and *kf* in the red spots of mimetic females were higher than those in the red spot-corresponding regions in non-mimetic females (Table 1). The expression levels of NBAD pathway genes *TH*, *DDC*, and *ebony* were upregulated in the red region in mimetic females, supporting the above results of qRT-PCR analysis (Fig. 5); however, the differences were not statistically significant (Table 2). Certain genes involved in the process of melanization, including those induced by immune responses, were upregulated in the red region in mimetic females (Table 1). *Prophenoloxidase 45* (*proPO 45*) and *yellow-d2* which are involved in the melanization process, were induced in the red region in mimetic females.

We also found that genes involved in the *Toll* signaling pathway, such as *snake*, *spatzle 5*, and *gastrulation-defective*, were upregulated in the red region of mimetic females (Table 1). *Toll* signaling activates

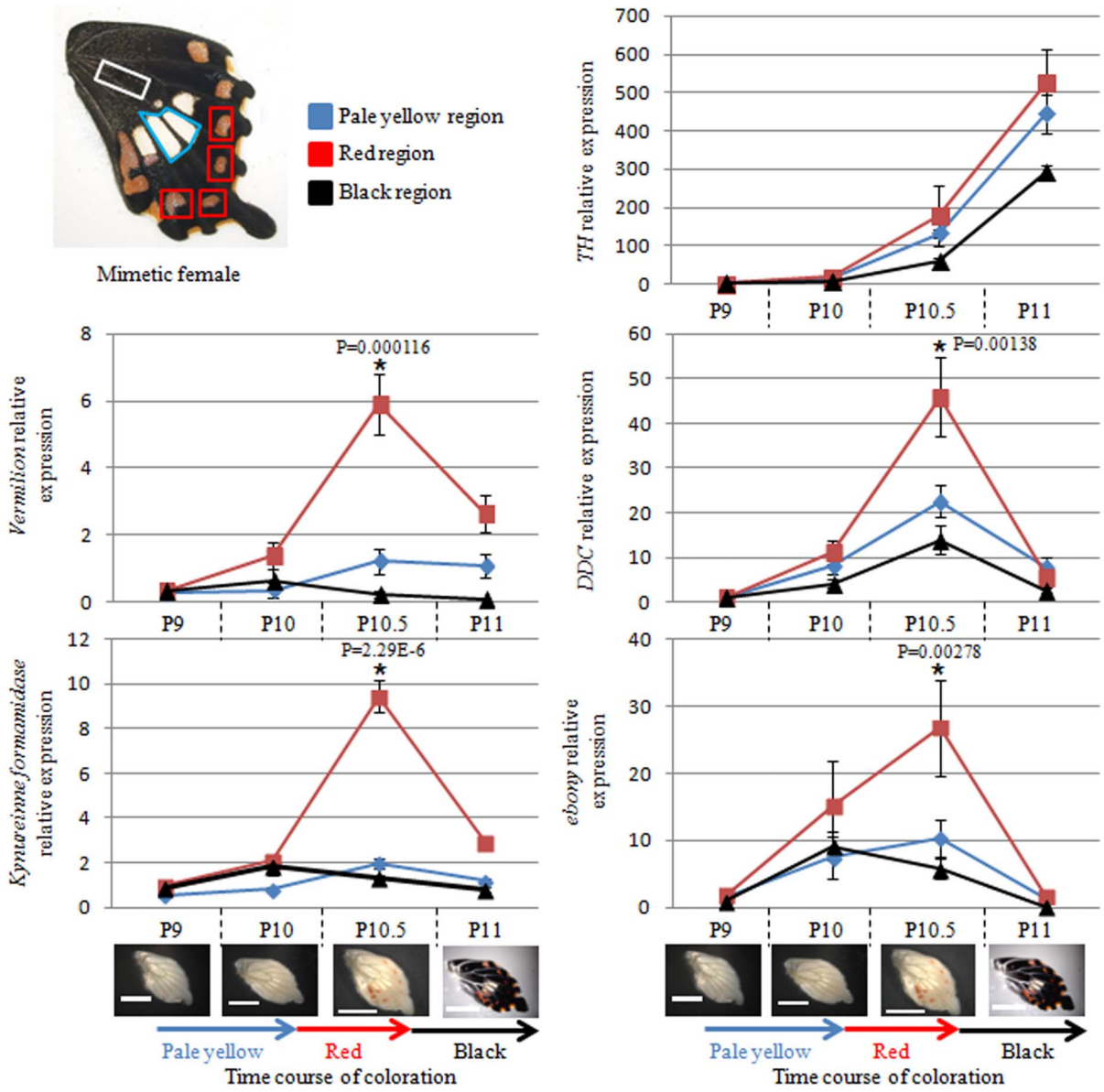

Figure 5 | Expression levels of kynurenine and NBAD pathway genes in the late pupal wings of mimetic females. Three separate regions are indicated: blue line, indicating the pale yellow region; red line, indicating the red spots; and black line, indicating the black region. The expression levels of all genes are shown relative to that of the *rpL3* control. Error bars show standard deviation of 3 experimental replicates. (*P < 0.01, one-way ANOVA). All images in this figure were captured by the author (H. Nishikawa).

the melanization process during an immune response[25]; thus, the red pigment in mimetic females may be synthesized by a process similar to that of melanin synthesis.

Discussion

In this study, we found that the pale yellow pigments in the wings of non-mimetic females of *P. polytes* are composed of kynurenine and NBAD (Fig. 3), which appear to form papiliochrome II (peak 1) and its related pigments (peaks 2 and 3). In papiliochrome II, the beta carbon of the side chain of NBAD is chemically linked to the amino group of kynurenine[17]. On the basis of their molecular weights, peak 2 (m/z 653.2933, Fig. 3c) was assumed to be a compound comprising kynurenine and an NBAD dimer and peak 3 (m/z 875.3944, Fig. 3d) was assumed to be a compound comprising kynurenine and an NBAD trimer. The pale yellow regions were also observed in the wings of mimetic female, but papiliochrome II and its related pigments were not observed (Fig. S4). Additionally, the expressions of genes involved in kynurenine and NBAD synthesis was upregulated in the pale yellow regions in non-mimetic females, but not in the pale yellow regions of mimetic females. These results suggest that papiliochrome II and its related pigments and the relevant biosynthetic genes are activated only in the pale yellow regions in non-mimetic females.

In *P. polytes*, male butterflies have been suggested to prefer non-mimetic females over mimetic females[26]. In another butterfly, *Pieris rapae*, Obara and Hidaka (1968)[27] reported that the difference in the reflection of ultraviolet light affects the mate choice. Papiliochrome II is known to reflect ultraviolet light[28], and thus, we can speculate that papiliochrome II and its related pigments in non-mimetic female wings contribute to mate choice in *P. polytes*. In mimetic females, papiliochrome II synthesis appeared to be reduced, which may result in reducing the male preference. Despite reduced male preference, mimetic females that switch the region-specific expression of the pale yellow pigments would succeed in enhancing the mimicry effect and protecting themselves from predators. It is intriguing that this type of trade-off can be explained by a switch of pigment synthesis.

Table 1 | Transcriptional changes of the selected genes in the red pigment synthesizing stage

Gene	Gene ontology	RPKM value		Fold change	q value
		red region	red spot corresponding region		
snake	*Toll* signaling pathway	1.39	0.03	51.47	6.16E-07
spatzle 5	*Toll* signaling pathway	8.26	0.02	394.49	3.99E-05
gastrulation-defective	*Toll* signaling pathway	3.05	0.11	27.11	0.049352
prophenoloxidase 45	dopamine metabolic process	34.57	3.81	9.06	0.048507
yellow-d2	melanin biosynthetic process	33.54	1.99	16.90	9.27E-08
vermilion	catabolic process to kynurenine	185.62	32.10	5.78	3.42E-07
Kynurenine formamidase	catabolic process to kynurenine	220.25	46.43	4.74	2.12E-05

RPKM, reads per kb of exons per million mapped reads; mimetic, red region of the hindwing of mimetic female; non-mimetic, red homologous region of the hindwing of non-mimetic female; Fold change, RPKM value of mimetic/RPKM value of non-mimetic.

In *P. polytes*, the *H* gene is known to be responsible for the development of the mimetic form[13] and controls not only the switch in the wing pattern but also the flight behavior of mimetic females[29]. Although the *H* gene has not been identified yet, this study demonstrated that expression of kynurenine and NBAD pathway genes (Fig. 4 and 5) and several other genes (Table 1, 2, S2, and S3) is strongly altered. In heliconid butterflies, the black region at the center of the forewing is determined by *WntA*[30,31] and the forewing band pattern is determined by *optix*[32]. In *P. polytes*, the *H* gene itself or transcription factors downstream of the *H* gene may control the pigment synthesis pathway and its region-specific expression.

The qRT-PCR and RNA sequencing analyses demonstrated that NBAD and kynurenine pathways are involved in red pigment synthesis in mimetic wings. We found that the chemical property of the red pigment was similar to that of the black pigment melanin, which is insoluble in hydrochloric acid (Fig. S7) and many organic solvents (data not shown). Melanin is considered to be a mixed polymer comprising indoles such as 5,6-dihydroxyindole-2-carboxylic acid and 5,6-dihydroxyindole in addition to variable amounts of other precursors in the synthesis pathway[23]. Unlike melanin synthesis, red pigment synthesis may use NBAD and kynurenine as the precursor substrates for polymerization.

Furthermore, multiple genes involved in the *Toll* signaling pathway, such as *snake*, *spatzle 5*, and *gastrulation-defective*, were upregulated in the red spots in mimetic females. *Toll* signaling pathway is involved in the immune response to bacterial or fungal infection[33,34] and in the formation of the dorsoventral axis[35]. In *D. melanogaster*, 6 types of *spatzle* genes have been identified; however, the functionis known only for *spatzle 1*. Spatzle 1 function is known as a ligand of the Toll receptor. It is processed into its active form by a serine protease cascade involved in gastrulation-defective and snake. After dimerization, the homodimer of spatzle 1 binds to the Toll receptor and activates the *Toll* signaling pathway. In addition to *Toll* signaling, activation of phenoloxidase and *yellow* genes is required for the melanization reaction during the immune response[25]. The upregulation of *Toll* signaling and melanization genes in the red regions in mimetic females implies that the formation of the red pigments in mimetic females mediated by a biosynthetic pathway analogous to melanization. First, a *Toll* signaling-like pathway is activated by the ligand molecule Spatzle 5 and its partner, an unknown Toll receptor from the dozen or so members of the *Toll* family in a region-specific manner. This process induces the expression of *proPO 45* and *yellow-d2*, which promotes polymerization of kynurenine and NBAD substrates that are activated simultaneously. In heliconid butterflies, an ocular pigment biosynthetic pathway (e.g., the one involving ommochrome synthesis genes such as *vermilion* and *cinnabar*[20]) produces the red or yellow coloration of the wings[32]. In contrast, in the red pigment synthesis in *P. polytes* wings, a different gene network, analogous to the immune response pathway, may have been recruited for red pigmentation during evolution.

Here we showed that the gene networks involved in color pattern formation are altered even between the similar pale yellow regions in mimetic and non-mimetic females. In addition, we demonstrated that both kynurenine and NBAD pathway networks are used in the pale yellow region of non-mimetic wings and the red region of mimetic wings, although their temporal and spatial expression profiles are controlled differently. These drastic changes are possibly regulated directly or indirectly by the *H* gene, the most upstream gene. Because *H/h* males do not show mimetic phenotypes, the *H* gene appears to be functional in producing mimetic wing coloration only in females. This observation is suggestive of the involvement of the *H* gene in sex differentiation pathways in later developmental stages. Identifying the *H* gene itself should help address the crosstalk between the sex differentiation pathway and the gene networks involved in changes of wing coloration in mimetic females.

Methods

Experimental animals. *P. polytes* was purchased from Eiko-Kagaku (Osaka, Japan) or Chokan-kabira (Okinawa, Japan). Larvae were reared on the leaves of *Citrus unsyiu* (Rutaceae) or on an artificial diet (Insecta LFM, NOSAN) including *Citrus* leaves powder under long day conditions (L : D = 16 h : 8 h) at 25°C. Pupal samples were staged by the length of time after pupal ecdysis.

Extraction of the pale yellow pigments from female hindwings. The pale yellow regions were dissected from the hindwings of 10 adults and added to 500 μL of 70% methanol. The supernatant containing the pale yellow pigment was completely evaporated and re-dissolved in water. This sample was centrifuged at 15000 rpm for 10 min to remove insoluble components and the supernatant was used in the experiments described below.

Table 2 | Transcriptional changes of NBAD synthesis pathway genes

Gene	Gene ontology	RPKM value		Fold change	q value
		red region	red spot corresponding region		
TH	melanin biosynthetic process from tyrosine	4690.75	3112.43	1.51	0.86692
DDC	melanin biosynthetic process from tyrosine	174.56	72.10	2.42	0.08456
ebony	melanin biosynthetic process from tyrosine	643.04	348.33	1.85	0.69866

RPKM value shows mean RPKM values of three replicates in each region. Fold change represents the ratio of RPKM value of mimetic female/that of non-mimetic female.

HPLC-ESI-MS. An HPLC system (Ultimate 3000, Dionex) was used for analysis. The autosampler tray and the column oven were maintained at 4°C and 45°C respectively. Chromatographic separation was performed on a 2.0 mm i.d. × 100 mm column (CD-C18, Cadenza). The elution gradient was based on a binary solvent system [time in min (% eluent A/% eluent B): 0 min (95/5); 1 min (95/5); 5 min (5/95); 10 min (5/95); 10.1 min (95/5); 20 min (95/5)]. Solvent A consisted of 0.1% formic acid in water and solvent B consisted of 0.1% formic acid in methanol. The flow rate was constant at 0.25 mL/min. The mobile phase was directly delivered to the ESI ion source. The compounds were analyzed on an ESI-Qq-TOF mass spectrometer (micrOTOFQ II, Bruker Daltonics). The source was operated in the positive ion mode.

Cloning of genes involved in kynurenine and NBAD synthesis. The sequences of *vermilion*, *TH*, *DDC*, and *ebony* were obtained from GenBank. Their accession numbers are AK405309, AB525743, AB525744, and AB525746, respectively. Degenerate oligonucleotide primers were designed on the basis of sequences of other insects such as *D. melanogaster*, *Tribolium castaneum* and *H. melpomene*. The primers were 5′-CTNGAGAGGGARYACTCTCCAAGCATGTGGTC-3′ and 5′-AATTCSCGCAAATCASANACGCCNGATAT-3′ for *kf*. The cycling conditions for PCR were 35 cycles of 95°C for 2 min, 49°C for 0.5 min, and 72°C for 1 min. PCR products were isolated, subcloned into a TA cloning vector (pGEM-T Easy vector, Promega), and sequenced on an ABI PRISM® 3100 Genetic Analyzer (ABI, USA).

Phylogenetic analysis. Sequences were aligned using ClustalX[36]. Phylogenetic trees were constructed by the neighbor-joining method in the MEGA5 software[37]. The confidence level of various phylogenetic lineages was assessed by bootstrap analysis. We also compared several related genes using phylogenetic analysis. The following sequences were used to create the phylogenetic tree: *Hm*, *H. melpomene* (GQ183897); *Tc*, *T. castaneum* (XM_962551); *Dm*, *D. melanogaster* (FBgn0031821); *Aa*, *Aedes aegypti* (DQ440173); and *Cq*, *Culex quinquefasciatus* (XM_001842738). The sequences of *kf* of *Hm*, *Tc*, *Aa*, and *Cq* were obtained from GenBank and that of *kf* and *Dm* was obtained from Flybase. Accession number of the *kf* gene in *Papilio polytes* was registered as AB857712.

qRT-PCR. The pupal wings were dissected (in cold phosphate-buffered saline, pH = 6.8) to isolate distinct parts: future black regions, future red regions, and future pale yellow regions in non-mimetic (Fig. 4) and mimetic (Fig. 5) females at the stages that correspond to 9–11 days after pupation (P9, P10, P10.5, and P11). We used 3–4 pupae for qRT-PCR assays at each stage: 3 pupae from each stage except for stage P10 of non-mimetic females (4 pupae). Wing tissue was either immediately transferred to cold TRI reagent (Sigma) and homogenized for RNA extraction or stored at −20°C before RNA extraction. The samples were treated with DNase I (TaKaRa) to remove the genomic DNA, followed by phenol-chloroform extraction and ethanol precipitation. Thereafter, RNA was dissolved in water and reverse-transcribed with random primers (N_6) using a first-strand cDNA synthesis kit (GE Healthcare). Real-time PCR was performed using Power SYBR Green PCR Master Mix on a StepOne system (Applied Biosystems Inc.). PCR was performed using these cycling condtions: at 95°C for 10 min, followed by 40 cycles of 95°C for 15 s, and 60°C for 60 s. Ribosomal protein L3 (*rpL3*) was used as an internal control. Expression levels of these genes were normalized to that of *rpL3*. Statistical analysis was performed using one-way ANOVA at each stage. To evaluate significant differences, the region in which the gene was differentially expressed was tested using Bonferroni correction. The sequences of the primer sets are listed in Table S1.

RNA sequencing. We used 3 pupae of each type (mimetic and non-mimetic females). The pupal hindwings were dissected to prepare the red region in mimetic females (Fig. 5, red region) and the red spot-corresponding region in non-mimetic females (Fig. 4, red spot-corresponding region) at P10.5. Total RNA was isolated as described above and purified using an RNeasy column (Qiagen). We prepared cDNA libraries ligated using different adaptor indices (total 6 libraries were created) according to the vendor's instructions (TruSeq RNA sample preparation, the low throughput protocol, Illumina). In brief, magnetic beads containing poly-T molecules were used to purify mRNA from 1 μg of total RNA. Purified mRNA was then fragmented chemically and reverse-transcribed into cDNA. Finally, end repair and A-tailing were performed before Illumina adapters were ligated to the cDNA fragments. These samples were used to amplify cDNA in 10 PCR cycles. The amplicons were validated using an Agilent 2100 bioanalyzer and Agilent High Sensitivity DNA kit (Agilent Technologies) and quantified using KAPA quantification. Each cDNA library was diluted to 2 nM. cDNA libraries were sequenced on the Illumina HiSeq 2000 using HiSeq v1 flow cells and sequencing chemistry. The accession numbers of all raw reads in RNA sequencing were as follows: the red regions in mimetic females (DRR014115, DRR014116, and DRR014117), the red spot-corresponding regions in non-mimetic female (DRR014118, DRR014119, and DRR014120).

To construct the assembled transcriptome, all raw reads were assembled using the Trinity (http://trinityrnaseq.sourceforge.net/)[38] *de novo* transcriptome assembly software packages. All reads of each library were mapped separately against the transcriptome sequences using the Bowtie 2, version2.1.0, (http://bowtie-bio.sourceforge.net/bowtie2/index.shtml) short-read aligner[39]. Transcript expression levels were estimated to calculate RPKM values. To identify genes differentially expressed in the 2 regions, we performed edgeR with iDEGES/edgeR using TCC version 1.0.0 of the R package. Assembled transcripts that were upregulated on the basis of edgeR with iDEGES/edgeR in both regions were annotated in the BLASTX software against *D. melanogaster* transcriptome sequences in Flybase (http://flybase.org/blast/) with an *E* value cut off of 0.001. Genes with *E* values of > 0.001 were annotated again in BLASTX against the NCBI nonredundant protein sequence database, with an *E* value cutoff of 0.001.

1. Nishida, R. & Fukami, H. Ecological adaptation of an Aristolochiaceae-feeding swallowtail butterfly, *Atrophaneura alcinous*, to aristolochic acids. *J. chem. Ecol.* **15**, 2549–2563 (1989).
2. Wray, V., David, R. H. & Nahrstedt, A. Biosynthesis of cyanogenic glycosides in butterflies and moths: incorporation of valine and isoleucine into linamarin and lotaustralin by *Zygaena* and *Heliconius* species (Lepidoptera). *Z. Naturforsch.* **38**, 583–588 (1983).
3. Nijhout, H. F. *The Analysis of Wing Patterns.* In The development and evolution of butterfly wing patterns. (Nijhout, H. F. ed.) 51–84 (Smithsonian Institution Press, Washington and London, 1991).
4. Muller, F. Ueber die Vortheile der Mimicry bei Schmetterlingen. *Zoologischer Anzeiger.* **1**, 54–55 (1878).
5. Brower, J. V. Z. Experimental studies of mimicry in some North American butterflies. Part I. The monarch, *Danaus plexippus* and viceroy *Limenitis archippus*. *Evolution* **12**, 32–47 (1958).
6. Brower, J. V. Z. Experimental studies of mimicry in some North American butterflies. Part II. *Battus philenor* and *Papilio troilus, P. polyxenes* and *P. glaucus*. *Evolution* **12**, 123–136 (1958).
7. Brower, J. V. Z. Experimental studies of mimicry in some North American butterflies. Part III. *Danaus gilippus berenice* and *Limenitis archippus floridensis*. *Evolution* **12**, 273–285 (1958).
8. Uesugi, K. The adaptive significance of Batesian mimicry in the swallowtail butterfly, Papilio polytes (Insecta, Papilionidae): associative learning in a predator. *Ethology* **102**, 762–775 (1996).
9. Jiggins, C. D. *et al.* A genetic linkage map of the mimetic butterfly *Heliconius melpomene*. *Genetics* **171**, 557–70 (2005).
10. Kapan, D. D. *et al.* Localization of Müllerian mimicry genes on a dense linkage map of *Heliconius erato*. *Genetics* **173**, 735–57 (2006).
11. Clarke, C. A. & Sheppard, P. M. The genetics of *Papilio dardanus* Brown. I. Race cenea from South Africa. *Genetics* **44**, 1347–1358 (1959).
12. Clarke, C. A. & Sheppard, P. M. The genetics of the mimetic butterfly *Papilio Glaucus*. *Ecology* **43**, 159–161 (1962).
13. Clarke, C. A. & Sheppard, P. M. The genetics of the mimetic butterfly *Papilio polytes* L. *Philosophical Transactions of the Royal Society of London. Series B, Biological Sciences* **263**, 431–458 (1972).
14. Morehouse, N. I., Vukusic, P. & Rutowski, R. Pterin pigment granules are responsible for both broadband light scattering and wavelength selective absorption in the wing scales of *pierid* butterflies. *Proc. Biol. Sci.* **274**, 359–66 (2007).
15. Koch, P. B. Precursors of pattern specific ommatin in red wing scales of the polyphenic butterfly *Araschnia levana* L.: Haemolymph tryptophan and 3-hydroxykynurenine. *Insect Biochem.* **21**, 785–794 (1991).
16. Reed, R. D. & Nagy, L. M. Evolutionary redeployment of a biosynthetic module: expression of eye pigment genes *vermilion*, *cinnabar*, and *white* in butterfly wing development. *Evol. Dev.* **7**, 301–11 (2005).
17. Rembold, H. & Umebachi, Y. *The structure of papiliochrome II, the yellow wing pigment of the Papilionid butterflies.* In Progress in Tryptophan and Serotonin Research. (Schlossberger, H. G., Kochen, W., Linzen, B. & Steinhart, H. ed.) 743–746 (Walter de Gruyter, Berlin, 1984).
18. Umebachi, Y. Distribution of papiliochrome in *Papilionid* butterflies. *The science reports of the Kanazawa university* **22**, 187–195 (1977).
19. Fujiwara, H. & Ogai, S. Ecdysteroid-induced programmed cell death and cell proliferation during pupal wing development of the silkworm, *Bombyx mori*. *Dev. Genes Evol.* **211**, 118–23 (2001).
20. Ferguson, L. C. & Jiggins, C. D. Shared and divergent expression domains on mimetic *Heliconius* wings. *Evol Dev.* **11**, 498–512 (2009).
21. Wittkopp, P. J., True, J. R. & Carroll, S. B. Reciprocal functions of the *Drosophila yellow* and *ebony* proteins in the development and evolution of pigment patterns. *Development* **129**, 1849–58 (2002).
22. Kramer, k. & Hopkins, T. L. Tyrosine Metabolism for Insect Cuticle Tanning. *Arch. Insect Biol. Phisiol.* **6**, 279–301 (1987).
23. True, J. R. Insect melanism the molecules matter. *Trends in ecology & evolution* **18**, 640–647 (2003).
24. Fogal, W. & Fraenkel, G. Melanin in the puparium and adult integument of the fleshfly, *Sarcophaga bullata*. *J. Insect Physiol.* **15**, 1437–1447 (1969).
25. Tanji, T., Hu, X., Weber, A. N. & Tony, Y. T. Toll and IMD pathways synergistically activate an innate immune response in *Drosophila melanogaster*. *Mol. Cell Biol.* **27**, 4578–88 (2007).
26. Ohsaki, N. A common mechanism explaining the evolution of female-limited and both-sex Batesian mimicry in butterflies. *J. Animal Ecology* **74**, 728–734 (2005).
27. Obara, Y. & Hidaka, T. Recognition of the female by the male, on the basis of ultra-violet reflection, in the white cabbage butterfly, *Pieris rapae crucivora* Boisduval. *Proc. Japan Acad.* **44**, 829–832 (1968).
28. Umebachi, Y. Papiliochrome, a new pigment group of butterfly. *Zoological Sci.* **2**, 163–174 (1985).

29. Kitamura, T. & Imafuku, M. Behavioral Batesian mimicry involving intraspecific polymorphism in the butterfly *Papilio polytes*. *Zoological Sci.* **27**, 217–21 (2010).
30. Martin, A. *et al.* Diversification of complex butterfly wing patterns by repeated regulatory evolution of a Wnt ligand. *Proc. Natl. Acad. Sci. U S A.* **109**, 12632–12637 (2012).
31. Papa, R. *et al.* Multi-allelic major effect genes interact with minor effect QTLs to control adaptive color pattern variation in *Heliconius erato*. *PLoS One* **8**, e57033 (2013).
32. Reed, R. D. *et al. optix* drives the repeated convergent evolution of butterfly wing pattern mimicry. *Science* **333**, 1137–41 (2011).
33. Lemaitre, B. & Hoffmann, J. The host defense of *Drosophila melanogaster*. *Annu. Rev. Immunol.* **25**, 697–743 (2007).
34. Valanne, S., Wang, J. H. & Rämet, M. The *Drosophila* Toll signaling pathway. *J. Immunol.* **186**, 649–56 (2011).
35. Ferrandon, D., Imler, J. L. & Hoffmann, J. A. Sensing infection in *Drosophila*: Toll and beyond. *Semin. Immunol.* **16**, 43–53 (2004).
36. Thompson, J. D., Gibson, T. J., Plewniak, F., Jeanmougin, F. & Higgins, D. G. The ClustalX windows interface: flexible strategies for multiple sequence alignment aided by quality analysis tools. *Nucleic Acids Research* **24**, 4876–4882 (1997).
37. Tamura, K. *et al.* MEGA5: Molecular evolutionary genetics analysis using maximum likelihood, evolutionary distance, and maximum parsimony methods. *Mol. Biol. Evol.* **28**, 2731–2739 (2011).
38. Grabherr, M. G. *et al.* Full-length transcriptome assembly from RNA-Seq data without a reference genome. *Nat. Biotechnol.* **29**, 644–52 (2011).
39. Langmead, B. & Salzberg, S. L. Fast gapped-read alignment with Bowtie 2. *Nat. Methods* **9**, 357–9 (2012).

Acknowledgments

We thank Jouji Seta (Bruker Daltonics K.K.) for the help in measuring the accurate mass spectrometry of the pale yellow pigments. We also thank to Dr. Tetsuya Kojima, Dr. Hiroshi Hori, and Dr. Ryo Futahashi for helpful comments. This work was supported by a Grant-in-aid for Scientific Research on Innovative Areas, "Genetic Bases for the Evolution of Complex Adaptive Traits", to H.F. (22128005) and MEXT KAKENHI Grant number 221S0002 to H.F.

Author contributions

H.N. performed most of experiments, with the assistance of M.I., K.S. and H.K. for LC/MS analysis, Y.S. and S.S. for RNA-sequencing, J.Y. supported data analysis of RNA-sequencing. H.F. and H.N. designed and interpreted experiments, and wrote the manuscripts.

Additional information

Supplementary information accompanies this paper at http://www.nature.com/scientificreports

Competing financial interests: The authors declare no competing financial interests.

How to cite this article: Nishikawa, H. *et al.* Molecular basis of wing coloration in a Batesian mimic butterfly, *Papilio polytes*. *Sci. Rep.* **3**, 3184; DOI:10.1038/srep03184 (2013).